FINAL REPORT

FOR CONTRACT NASW-4814

CORONAL ABUNDANCES AND THEIR VARIATION

Date: 12 December 1996

Principal Investigator:

Julia L.R. Saba (Lockheed Martin Organization H1-1C)

Local address (Lockheed Martin Remote Site):

Code 682.3, NASA/Goddard Space Flight Center
Greenbelt, Maryland 20771

Institution address:

Lockheed Martin Palo Alto Research Laboratory
Organization H1-12, Building 252
3251 Hanover Street
Palo Alto, California 93404

ABSTRACT

This contract supported the investigation of elemental abundances in the solar corona, principally through analysis of high-resolution soft X-ray spectra from the Flat Crystal Spectrometer on NASA's Solar Maximum Mission. The goals of the study were a characterization of the mean values of relative abundances of elements accessible in the FCS data, and information on the extent and circumstances of their variability. This is the Final Report, summarizing the data analysis and reporting activities which occurred during the period of performance, June 1993 - December 1996.

Subject terms: Solar corona, X-ray spectra, elemental abundances, abundance variability

FINAL REPORT FOR CONTRACT NASW-4814

CORONAL ABUNDANCES AND THEIR VARIATION

INTRODUCTION

This is the final report for contract NASW-4814. The contract resulted from an award under NASA's Supporting Research & Technology Program after peer review of a proposal submitted by the Principal Investigator (PI) in August 1992 in response to NASA Reseach Announcement NRA-92-OSSA-10. Notification of the award was given in February 1993 and funding began in June 1993. The current investigation is a continuation and an extension of a pilot study of coronal abundances begun as a Solar Maximum Mission Guest Investigation (GI) by the same PI. The original period of performance was three years. A six-month, no-cost extension to December 1996 was granted to allow comparison of the study results with those from the Yohkoh and SOHO instruments, and formulation of recommendations of new measurements that need to be made to confirm results of the study and to answer outstanding questions. In the last year of the study, an ongoing informal collaboration with Dr. Joan Schmelz was formalized with a subcontract from Lockheed Martin, the PI's institution, to the University of Memphis, to allow Dr. Schmelz to charge to the contract. Bringing Dr. Schmelz into the project has helped offset the overhead rate increase at the PI's institution after the contract was awarded.

The contract supported an investigation of elemental abundances in the outer atmosphere of the Sun, principally through analysis of high-resolution soft X-ray spectra from the Flat Crystal Spectrometer (FCS) on the Solar Maximum Mission (SMM), a NASA mission dedicated to solar observations from 1980 through 1989. This instrument acquired excellent spectral data for studying the relative amounts of oxygen, neon, magnesium, and iron in solar active regions.

The project included analysis of this data base to decouple the effects of temperature and abundance, to assess different theoretical calculations of spectral line intensities for use in the study, and to account for the possible effects of opacity due to resonance scattering. The primary goals of the study were a characterization of the mean values of relative abundances of elements accessible in the FCS data and information on the extent and circumstances of their variability.

CONTENTS OF REPORT

This report contains an introductory section, a section giving a verbal outline of the report contents, a scientific background section, a results section, a section on lessons learned and recommendations to NASA and other investigators, lists of publications supported by the contract, and meeting reports of the study results, a list of references, one table, and five figures at the end, preceded by captions extracted from the text.

The organization of the first three subsections of the Results portion of this report conforms roughly to the outline of the contract statement of work. The fourth Results subsection discusses comparison of FCS results with results from other instruments, which was made possible by the contract extension.

BACKGROUND

Knowledge of solar elemental abundances is essential for correct interpretation of plasma diagnostic information from spectral and image data. Also, an assumed set of abundances is implicit in many aspects of astrophysical data analysis, such as calculations of energetics and radiative loss rates, and comparisons of relative emission in different wavebands to assess possible emission mechanisms.

Solar coronal elemental abundances are now known to differ from their photospheric counterparts. Evidence comes from both in situ measurements of solar energetic particles (SEP) and X-ray and EUV spectroscopic observations of coronal plasma. The atomic property that best correlates with these photospheric/coronal abundance differences is the First Ionization Potential (FIP) of the element. In addition, there is a growing body of observational evidence that coronal abundances vary under different physical conditions. Systematic differences in the average composition of the corona compared to the photosphere, and details of coronal abundance variability might give important clues to the fundamental problems of coronal heating and mass supply.

A graphic illustration of coronal abundance variation is given in Figure 1, which shows two examples of the lowest energy FCS spectrum for two different solar active regions during periods of queiscence. The regions have very similar temperatures (about Log T = 6.5) as determined from the ratio of the Fe XVIII line at 14.22 A (line (d) in upper plot) to the Fe XVII line at 16.78 A (not shown). The strengths of the spectral lines are very similar in each spectrum except for the three lines from the helium-like neon triplet at the far left, denoted (a), (b), and (c) in the upper plot. Those in the first spectrum are significantly stronger than their counterparts in the second spectrum. Several possible explanations for the observed flux differences (which did not involve abundance variations) were investigated but eliminated as the possible source of the flux differences. Only Fe/Ne abundance variations of at least a factor of four in active regions (Strong et al. 1991) gave a satisfactory explanation. This figure and its implications sparked the FCS abundance investigation described in this report.

One important question related to Figure 1 is whether it is the iron or the neon abundance (or both) that is varying in these active regions. The figure gives the impression that it is neon that changes, but the scientific opinion of various experts in the field of abundances argued otherwise. Several pieces of evidence, the strongest coming from the SEP results of Reames (1995), suggested a normalization of the trace elements with respect to hydrogen (which makes up the bulk of the coronal plasma) such that the low-FIP elements (with FIP < 10 eV) were enhanced by about a factor of four over their photospheric counterparts while the high-FIP elements (FIP > 11 eV) were the same in the photosphere and the corona. (This normalization is controversial and will be discussed later in this report, in section 4. of the Results.) In the strictest interpretation of this empirical model, the abundance of neon could not vary under any conditions. As described later in this report, our results contradict this interpretation.

RESULTS OF THE FCS ACTIVE REGION ABUNDANCE STUDY

1. ANALYSIS TOOLS

a. Fe XVII Resonance Scattering

Based on the preliminary results reported by Schmelz, Saba, & Strong (1992), we had high hopes that resonance scattering of the Fe XVII line at 15.01 A might be used as a new density diagnostic tool in our analysis. Assessing its possible use involved two areas of investigation: (1) confirmation that measurable resonance scattering is in fact occurring, and (2) careful re-examination of the steps made in deriving electron densities from the observed resonance scattering effects.

(1) We have confirmed that FCS spectroscopic analysis is consistent with significant resonance scattering for the 15.01-A line of Fe XVII under normal active region conditions. For the cores of bright active regions, our results suggest that photons are scattered out of the line of sight, reducing the measured line intensities to about half of that predicted. We have found no reaonable explanation for the depleted flux other than resonance scattering, particularly since other bright Fe XVII lines not expected to be so affected by scattering are well modeled by recent emissivity calculations (see section 1.b) while the 15.01-A line is not. The interpretation of resonance scattering is reinforced by the finding of a weak center-to-limb effect (Schmelz et al. 1997), in the sense that regions close to the limb appear to show more scattering. Such a trend is in keeping with expectations of longer lines-of-sight at the limb, and also with historical reports of resonance scattering of some cooler EUV lines. Figure 2a shows the flux ratio of the unaffected 16.78-A line of Fe XVII to the most-affected 15.01-A line for the FCS data (crosses) and the theoretical predictions (solid line for Log T = 6.5 and dashed lines for Log T = 6.4 and 6.6, a range which covers those found for the quiescent active regions in our study). The data points are plotted in order of increasing distance from Sun center and are all significantly above the expected theoretical values, consistent with 15.01-A photons being scattered out of the line of sight. For comparison, Figure 2b shows the same type of plot, with the 15.25-A line substituted for the 15.01-A line. The 15.25-A line has an opacity less than 25% that of the 15.01-A line, so it should not show significant opacity effects under normal active region conditions. The data and theory agree, indicating that these two lines are well explained with an optically thin approximation.

Note that the direction and magnitude of the center-to-limb effect we find for resonance scattering of Fe XVII at 15.01 A conflict with the recent results of Phillips et al. (1996) who, using some of the same FCS data, find a strong center-to-limb effect in the opposite sense; i.e., the scattering is more pronounced at disk center, and diminishes to near zero at the limb. The sense of their finding is not consistent with any previous reports of resonance scattering detection that we have seen. The analysis of Phillips et al. is complex, involving production of synthetic spectra for their sample of active regions and flares; the analysis method is noted but is not reproduced in the short paper they published describing the result. On the other hand, our analysis method is quite simple -- we compare measured ratios of the affected Fe XVII line at 15.01 A with the virtually unaffected Fe XVII line at 16.78 A, for quiescent active regions at various locations on the solar disk;

the predicted ratio is insensitive to temperature, and independent of elemental abundance and ionization fraction; we have ruled out obvious transient effects by our data selection process. After puzzling over this discrepancy for some time and attempting to reconcile the two results by discussion, we find that we cannot. After a careful reexamination of our own work and a sanity check based on some data from the Soft X-ray Telescope (SXT) on Yohkoh (see subsection 4.b in Results), we now have confidence that our result is correct and we will be publishing a detailed account of our analysis in a forthcoming paper on Fe XVII data/theory comparison by Saba et al. (1997).

(2) Unfortunately, even though we believe we have confirmed that resonance scattering is the best explanation for the discrepancy between the measured and optically thin prediction of the flux in the 15.01-A Fe XVII line, there are two (somewhat related) problems with a straightforward inferrence of the electron density from the measured flux reduction: (a) the resonance scattering process in the active region geometry needs to be modeled more exactly to derive the calculated opacity to an accuracy better than about a factor of two; and (b), in deriving the expression for electron density,

$$n_e \sim 4.84e\text{-}20\ EM/tau,$$

where n_e is the electron density, EM is the volume emission measure, and tau is the opacity derived from the measured reduction in 15.01-A flux (Schmelz, Saba, & Strong 1992), the required substitution of EM/n_e for the integrated column depth neglects a geometric term that is a combination of volume and line-of-sight filling factors. Although the method provides active region densities that are plausible, the results cannot be considered reliable at this time. The latter difficulty may be overcome to some extent by future observations which combine direct information on the appropriate geometric model from high-resolution imaging such as the subarsecond-pixel multilayer coronal images which the upcoming NASA Small Explorer TRACE (the Transition Region and Coronal Explorer) will provide. It is also desirable to have confirmation on the estimate of density from scattering through independent information on the electron density from a density-diagnostic line ratio, which must be appropriate for the temperature regime of the resonantly scattered line.

We note that we intend to follow up on this elusive but exciting possiblity in future work. We have recently begun working with Dr. Anand Bhatia (Goddard) and Dr. Sid Kastner in a NASA-sponsored opacity project which will compare resonance scattering in different simple geometric models with archival and recent EUV and soft X-ray data from solar active regions. We are attempting to identify promising EUV candidate lines for resonance scattering which can be studied jointly by the SoHO CDS and EIT instruments and by TRACE, and we are discussing with our SOHO and TRACE colleagues the specific coordinated measurements we need to make.

b. Excitation Rates for Fe XVII

New atomic data by Bhatia & Doschek (1992) and by Cornille et al. (1994) are consistent with the FCS active region data for Fe XVII at 15.25 A and 16.78 A, but apparently not with the 15.01-A line; the latter appears to show significant resonance scattering under normal active region conditions, as discussed above in section 1.a. The Fe XVII lines at 17.05 and 17.10 A are still under investigation.

The FCS results have been provided to Dr. Bhatia, and will be presented in the Fe XVII data/theory comparison paper by Saba et al. (1997). The 15.25-A line has an opacity 0.23 times as large as that of the 15.01-A line, while the 16.78-A line has an opacity that is less than 0.05 of the 15.01-A line. Hence we have generally used in our analysis the 16.78-A line, which our results show can be taken as optically thin under normal active region conditions.

c. Ionization Balance Calculations

The FCS spectroscopic results for active regions appear to be more easily understood if the ionization balance calculations of Arnaud & Rothenflug (1985) are used for Fe XVII and Fe XVIII rather than the newer results of Arnaud & Raymond (1992). This can be demonstrated in two ways:

(1) If Arnaud & Rothenflug (1985) ionization fractions for Fe XVII and Fe XVIII are used, in the temperature-diagnostic Fe XVIII/Fe XVII line ratios and in ratios of the Fe XVII lines with the Ne IX line, then the Fe/Ne abundances derived from FCS line ratios fall between the photospheric and coronal values as one might expect from a generalized FIP-based picure. On the other hand, if the Arnaud & Raymond (1992) calculations are used, then the FCS abundance ratios for Fe/Ne are primarily less than the photospheric value, which is troubling.

(2) For most quiescent active regions, an isothermal temperature distribution is implied for O VIII, Ne IX, and Mg XI, when Meyer (1985) abundances and emissivities tabulated by Mewe, Gronenschild, & van den Oord (1985) are used.

If atomic data from Bhatia & Doschek (1992) are used for the Fe XVII lines at 15.25 A and 16.78 A, and atomic data from McKenzie & Feldman (1992) for Fe XVIII at 14.22 A, an isothermal distribution results if the Arnaud & Rothenflug (1985) ionization fractions are used (for an iron abundance of 3.2e-5, the meteoritic value). This is shown in the top panel of Figure 3, where, for one of the FCS quiescent active region spectra, the one-sigma emission measure bands for the O VIII, Ne IX, and Mg XI resonance lines (all shown with dotted curves), and for the Fe XVII 16.78-A line (dot-dash curves) and the Fe XVIII 14.22-A line (dashed curves) all intersect in a single temperature solution. If the newer ionization fraction calculations of Arnaud & Raymond (1992) are used, the results are more complex, as shown in the bottom panel of Figure 3; in particular, no single isothermal solution can be found. While it is not expected that the coronal plasma above active regions is truly isothermal, it has been shown (Schmelz et al. 1996) that the plasma appears "effectively isothermal" in the soft X-ray regime if there is no concurrent transient activity. Further, for a few of the quiescent active region spectra, when the Arnaud & Raymond iron ion fractions are used, the Fe XVIII/Fe XVII temperature-diagnostic line ratio implies a temperature that is inconsistent with the upper limits of other FCS high-temperature lines.

2. UPDATED ACTIVE REGION ABUNDANCE STUDY:

a. Assessment of Resonance Scattering Impact on FCS Abundance Analysis

Because significant, variable resonance scattering affects the 15.01-A line of Fe XVII, we have omitted it from our upgraded abundance

analysis. This required redoing most of the analysis done in the SMM Guest Investigation of active region abundances, where the 15.01-A line was used extensively, because the line is the most intense and provides the best statistics. For our prime temperature-diagnostic line ratio, we had previously used the ratio of Fe XVIII at 14.22 A to the Fe XVII line at 15.01-A; this ratio was an extremely sensitive diagnostic, varying by two orders of magnitude over the active region range of temperatures of about 2-4 MK. In the new work we substitute the well-modeled, optically thin line of Fe XVII at 16.78 A for the 15.01-A line.

Besides requiring additional work, this substitution led to increased statistical uncertainties on temperatures derived in our analyses. More important, it greatly reduced our available sample of primary data to those spectral scans which included the 16.78-A line, and hence reduced our ability to carry out more extensive statistical and correlative studies. At an intermediate state in our analysis, when we were discussing opacity effects with Dr. Katrina Waljeski (NRL), it appeared that resonance scattering could play an even more important role, for other lines as well the 15.01-A line (cf. Waljeski et al. 1994). So we omitted from our choice of substitutes for the 15.01-A line the 15.25-A line of Fe XVII, which has about 0.25 the opacity of the 15.01-A line. We now believe that resonance scattering effects are more modest under typical active region conditions, and it might be possible to use the 15.25-A line without much concern over its introduction of extra scatter in the abundance variability results. This would expand the available data sample, since there are many FCS spectral scans which include the 15.25-A line, but not the 16.68-A line. However, for the present study we chose the more conservative course of using a line which is virtually unaffected by scattering for any reasonable active region conditions, since the reality of active region abundance variability was an issue.

b. Choice of Line Emissivities for Use in Analysis

(1) Ionization Balance Calculations

As discussed above in section 1.c, the use of the older Arnaud & Rothenflug (1985) ionization fractions for the Fe XVII and Fe XVIII lines used in this study make the results simpler to interpret than the newer calculations by Arnaud & Raymond (1992). That does not necessarily make them correct, but given all the other complications of the analysis, we decided to use the older calculations for most of the analysis. If nothing else, it may be more consistent to use them for the iron lines since we are already using using the Arnaud & Rothenflug (1985) ionization balance calculations for O VIII, Ne IX, and Mg XI lines, as we are unaware of any better set to use.

Where possible in our analysis, we have compared results from using the two different sets of ionization fractions for Fe XVII and Fe XVIII.

(2) Atomic data

Based on our examination of new atomic data for the several Fe XVII lines used in the study, we have adopted the distorted wave calculations of Bhatia & Doschek (1992). In general, their results are very comparable to the new calculations of Cornille et al. (1992). Where minor differences exist, we have chosen to use the Bhatia & Doschek results

because of our continuing close collaborative association with Dr. Bhatia, which makes it easier to make certain we are using the calculations correctly, and because Dr. Bhatia has kindly provided additional specific results evaluated at a variety of temperatures and densities as needed.

For the emissivities for resonance, intersystem, and forbidden lines of O VIII, Ne IX, and Mg XI, we have used the values tabulated by Mewe, Gronenschild, & van den Oord (1985), both because they were available in convenient, self-consistent form, and because we have no reason at this time to prefer any other calculations. For the Fe XVIII line at 14.22 A, we have used emissivities given in McKenzie & Feldman (1992).

c. Active Region Abundance Measurements

The quantitative results of our active region abundance study can be summarized as follows:

(1) In a sample of 33 FCS spectra from active regions in queiscent states, the mean values for Mg, Fe, and Ne abundances relative to O are given by:

Mg/O = 0.21 +/- 0.016, Fe/O = 0.106 +/- 0.004, Ne/O = 0.17 +/- 0.006, where the quoted uncertainties are the errors on the means, not the dispersions (Schmelz, Saba, & Islam 1997). The individual values for each spectrum are given in Table 1.

The average values can be compared with the SEP values reported by Reames (1995):

Mg/O = 0.19 +/- 0.004, Fe/O = 0.134 +/- 0.004, Ne/O = 0.152 +/- 0.004, where the quoted uncertainties are again errors on the means.

That is, our mean active region abundance value for Mg/O agrees with that of Reames (1995) determined from SEP data. Our respective mean values for Ne/O and Fe/O are not quite in agreement, although this could be due to the fairly limited sample of FCS quiescent active region spectra remaining after our strict filtering criteria, to remove multithermal effects that might masquerade as abundance variation.

(2) The dispersion in relative abundances is much greater in the FCS quiescent active region data sample than in the SEP data of Reames (1995), as can be seen from Figure 4. In the figure, the left panel shows the histogram distributions of Mg/O, Ne/O, and Fe/O for the SEP measurements of Reames (1995). (Note that the variance of the SEP Fe/O distribution is much larger than for Mg/O or Ne/O.) The right panel of Figure 4 gives the histogram distribution of relative abundances for the sample of 33 FCS spectra from quiescent active regions. A possible explanation emerging from our discussions with Dr. Don Reames (Goddard) is that the SEP data come from averages over larger spatial and temporal scales. The FCS data are sampled on an hour or less, with a 15-arcsec (FWHM) field of view. The SEP gradual event data are now thought to come from ambient coronal material swept up in large-scale ejections of ambient coronal material, which typically last several hours.

(3) In our quiescent active-region sample, about half of the time, the relative abundances for O:Ne:Mg:Fe are consistent with the "adopted coronal" abundances of Meyer (1985). In about half of the

cases, they are not.

(4) Fe/Ne relative abundances vary in active regions by at least a factor of four (discovered by Strong, Lemen, & Linford 1991; confirmed by Saba & Strong 1993, in initial study of the effect of ionization balance calculations used).

(5) The bounding values of the Fe/Ne ratio depend on the ionization balance calculation used for iron. For the Arnaud & Rothenflug (1985) iron ion fractions, the ratio varies roughly from the photospheric to the coronal value.

(6) The neon elemental abundance varies in quiescent active regions about 25% of the time (Schmelz et al. 1996). In some cases where Fe:Mg:O relative abundances are consistent with the "adopted coronal" values of Meyer (1985), Fe:Mg:O:Ne are not, suggesting that it is the neon which is anomalous in these cases. There are other types of variability as well.

(7) Ne/O ranges both above and below the nominal value of 0.15 by up to a factor of 2 in each direction. This finding, that neon can be both enhanced and depleted, is not consistent with current FIP-based models, and implies some additional differentiation mechanism, besides the ion-neutral separation presumed to operate in the upper chromosphere or the transition region, is at work at least some of the time.

3. MULTI-THERMAL ANALYSIS

a. Abundances Under Flaring Conditions

We did not offer to study abundance variations during the rapidly changing plasma conditions associated with actual flaring, since the FCS spectral scans are not in general well suited to such a study. (This is because each scan required 10 minutes or more to cover the desired wavelength range at a speed which allowed sufficient statistics to be accumulated in all of the lines needed, and the plasma conditions would be likely to change during a single scan so that information from the different lines could not be readily compared.) However, to understand the active region abundance variations, we have tried to use flare results from the FCS and the BCS as well as a previous gamma-ray result for context, in particular for the several detections of anomalous neon in quiescent active regions.

An abundance differentiation mechanism based solely on low-FIP enhancement would require that the neon abundance does not vary at all (with respect to hydrogen). The first strong evidence to suggest that the neon abundance deviated from the photospheric value was reported for two very different solar flares observed by SMM: (1) Gamma-Ray Spectrometer observations of an X5 limb flare on 1981 April 27 (Murphy et al. 1991) and (2) FCS observations of an impulsive double flare on 1980 November 5 (Schmelz & Fludra 1993). In both cases, the neon abundance (relative to both high-FIP and low-FIP heavy elements) was higher than the expected coronal value. The combination of the FIP differentiation expected from SEPs and chromospheric evaporation could not explain the high neon abundances observed for these two flares or the high argon abundances observed by Veck & Parkinson (1982).

Another mechanism (or mechanisms) superimposed on the basic FIP

differentiation model must be invoked to explain the enhanced neon or argon abundances. Shemi (1991) suggested that preflare soft X-ray radiation could penetrate deep into the solar atmosphere and create nonthermal ionization ratios at the base of the chromosphere. Because the photoionization cross section of neon (and argon) is high and the probability of recombination is low, ionized neon (and argon) could be selected along with the thermally ionized low-FIP elements for preferential transfer to higher levels of the solar atmosphere by the ion-neutral differentiating mechanism operating in the chromosphere. Therefore, the interaction region, i.e., the site of the plasma where the energetic particles and the ambient plasma interact during the flare, contains an over-abundance of ionized neon (and argon) with respect to other elements with high FIP. Shemi (1991) emphasized that the process of building up the neon (and argon) ions in the low solar atmosphere takes time. If photoionization is responsible for the enhanced neon (and argon) abundance, there must be an extended period of energetic soft X-ray emission. This condition was met for both neon-enhanced flares noted above: the 1981 April 27 flare was a long-duration event which lasted several hours in soft X-rays and the 1980 November 5 flare had a long and intense preflare phase.

However, it does not appear that similar conditions apply to the cases where enhanced neon (relative to oxygen, magnesium, and iron) occurs in quiescent active regions. Simultaneous data from the BCS shows no evidence of pronounced prolonged heating during or shortly before the time that the active region measurements were made. Enhancements or depletions of the high-FIP element neon outside of flares have not yet been explained by any model seeking to predict coronal elemental abundances.

b. Long-Duration Events

The FCS data base contains spectra from two interesting long-duration events (LDEs) from a flaring loop structure on the solar limb. One set of spectra was obtained at the loop footpoints, while the other was obtained at the peak of the loop. At the time the proposal for this project was written, it was thought that analysis of these two spectral data sets would provide a way to expand the abundance studies of quiescent active regions to a data set where the physical conditions were more dynamic, but not explosive. Unfortunately, one of the essential tools envisioned to analyze these data was not up to the task.

The XRP Differential Emission Measure (DEM) code "DEMON," which does an excellent job with the multi-thermal analysis of flaring soft X-ray plasma, did not work well with the LDE spectra because the plasma was too cool. While the FCS has multiple high-temperature lines to constrain the amount of high-temperature plasma in the field of view, it does not contain enough low-temperature lines to effectively constrain the low-temperature end of the plasma distribution; in DEM parlance, the DEM kernel is unstable and a proper inversion cannot be made. The lowest-temperature line available is the O VIII line at 18.97 A with a peak formation temperature of 3 MK. Although an effective low-temperature constraint for flaring plasma, it is not good enough for quiescent regions (whose temperature distribution typically peaks around 3 MK or even lower) and, as was learned from this study, also not good enough for a multi-thermal abundance analysis of LDEs. Unfortunately, without an effective method to determine the multi-thermal nature of the LDE plasma, it has been impossible to date to do true correlative studies of simultaneous data on abundances,

heating, and dynamics.

Nevertheless, we continue to believe that there are indirect grounds for expecting some such correlations in future studies: Saba & Strong (1991a,b) reported "nonthermal" soft X-ray line broadening which seemed to be associated with the soft X-ray cores in bright active regions; the largest excess velocities presumably occurred at the sites most recently heated. The FCS spectral scans used in this abundance study were taken at the brightest locations found in a pre-scan active region survey. The variances in the FCS relative abundance measurements are larger than those found in the SEP results of Reames (1995) (see section 2.c), which come from averages over larger spatial scales and longer time scales. The greater variation seen in the FCS data most probably reflects the finer sampling of a broad range of plasma conditions, including more dynamic sites which had recently undergone heating (although concurrent transient activity per se was excluded by our spectral stability criteria).

We are discussing with SOHO CDS, SOHO EIT, Yohkoh Soft X-ray Telescope (SXT) and TRACE colleagues the joint measurements needed to explore possible relationships between coronal abundance variations and coronal dynamics and heating. SXT and EIT could produce full-disk context images in several filters, or higher cadence images in ~2.5 arcsec pixels. TRACE could provide subarcsecond imaging of an active region in EUV filters somewhat comparable to EIT's, covering Fe IX/X, Fe XI/XII, and Fe XV at a cadence of seconds or less to track dynamics and the evolution of plasma heating. SXT would provide the best constraints on subflare emission hotter than about log T = 6.5. CDS would provide lines covering a broad range of tempratures, to determine the detailed temperature distribution of the plasma and the relative composition of heavy elements. It is imperative that CDS provide measurements of the hottest possible subflare lines, such as Fe XV, XVI, and XVII, as well as other fainter hot lines, to allow the maximum possible overlap with the SXT response.

c. High-Temperature Components

Fortunately, the very properties of the FCS that made the LDE project described above so difficult also made investigation of high-temperature components straightforward. The FCS had many high-temperature lines in its wavelength range so the fluxes (or limits on the fluxes) of these lines could be used to constrain the amount of high-temperature plasma in the instrument's field of view. In addition, the Bent Crystal Spectrometer (BCS) on SMM, an instrument used mainly to observe flaring plasma but also sensitive to smaller high-temperature transient events, was always pointed at the same active region as was the FCS. A detailed study of possible high-temperature components in the 33 sets of FCS long spectral scans made on quiescent active region targets was published in the paper by Schmelz et al. (1996). Five of these spectra showed evidence of hot plasma, all from small transient events.

Our preliminary analysis indicates that quiescent soft X-ray loops have a narrow temperature distribution that peaks between 2 and 3 MK and falls off sharply on either side. Confirmation of this result will require analysis of data having multiple spectral lines with peak formation temperatures which cover well at least the 1.5-6 MK temperature range. Since all of our active region spectra with high-temperature components involve transient events, we expect that characterization of this hotter component will require moderate-cadence,

arcsecond-pixel (or less) imaging as well as spectral scans with a cadence of at most a few minutes.

We are discussing with SOHO CDS, SOHO EIT, SXT and TRACE colleagues the joint measurements needed to make progress on high-temperature components in active region plasma. In another NASA-supported study, we are also attempting to use existing coordinated data taken by SXT (to constrain the high-temperature end of the plasma distribution) and the Goddard Solar EUV Rocket Telescope and Spectrograph (SERTS), which constrains the emission distribution over the approximate temperature range 1-3 MK.

4. Comparisons with Other Data Sets

We have attempted to compare results from our study with results from other instruments, to shed light on when abundances are found to vary, to provide a sanity check on our FCS resonance scattering results, and to see what can be learned about the absolute normalization of the coronal abundances relative to hydrogen, which provides the bulk of the coronal plasma. The last issue is one of the major unresolved questions in the coronal abundance arena; the normalization is needed to convert observed emission line intensities into useful estimates of the total amount of emitting material, a quantity that figures importantly, for example, in calculations of energetics and radiative cooling times.

The solar wind and SEP observations seem to imply that low-FIP elements are enhanced in the corona by a factor of 3 to 4, while the high-FIP elements have their photospheric values. However, a variety of acceleration and transport processes may treat protons (i.e., ionized hydrogen) differently than heavier atoms, so that heavy ion-to-proton ratios may not directly reflect the coronal heavy element-to-hydrogen composition. Hence it is desirable to have independent information from spectroscopic abundance measurements. Unfortunately, at present, the spectroscopic results are not consistent.

The usual way to derive the heavy element abundance normalization to hydrogen soft X-ray or EUV coronal spectroscopic data to is to compare line to continuum data when the continuum is dominated by free-free radiation. This is possible under some flaring conditions as observed with the SMM BCS and the Yohokoh BCS, but not with the FCS since the FCS continuum is contaminated with non-solar radiation. To date, the SMM BCS and Yohkoh BCS normalizations for the low-FIP calcium do not agree, and the Yohkoh BCS and SMM BCS experts (in some cases the same people) are trying to reconcile the differences. Generally, the SMM BCS absolute calcium abundances (Sylwester et al. 1996) appear higher than the Yokhoh BCS abundances, although careful study of one flare for which there was both BCS and FCS data suggested that calcium is enhanced only by about a factor of 2 rather than a factor of 4, that high-FIP elements are reduced by about a factor of 2, and that the normalization transition is more gradual than a low-FIP/ high-FIP step function between about 10 and 11 eV (Fludra & Schmelz 1995). Note that any contamination of the continuum would tend to reduce the derived calcium abundance. On the other hand, use of an empirical ionization fraction for Ca XIX might artificially enhance the calcium

With data from Yohkoh BCS, SMM BCS, and P78-1, Phillips et al. (1995) used ratios of Fe K-alpha and K-beta X-ray lines at 1.94 and 1.76 A (formed by fluorescence of neutral or near-neutral iron atoms) to the Fe XXV resonance line at 1.85 A, to deduce a ratio for the photosperic-

to-coronal abundance of iron near unity.

An FCS analysis based on resonance scattering in a limb region derived a coronal iron abundance at least 3 times greater than the photospheric value (Waljeski et al. 1994), although there are two major caveats to this result: (1) there is a tacit assumption of unit filling factor, which is probably invalid, and (2) a more thorough assessment of the same spectrum, using additional Fe XVII lines yields a very large uncertainty on the derived optical depth, which propagates to a large uncertainity on the abundance normalization.

a. SMM-FCS vs. SMM-BCS Abundance Variability

We have attempted to compare the FCS active region abundance data from our study with relevant SMM-BCS flare abundance results. In particular, we hoped to see if the "normal" or "anomalous" abundances in flares were correlated with "normal" or "anomalous" abundances in their parent active regions (although by definition the flare and quiescent active region data are not taken simultaneously). A detailed study of flare-to-flare variations of the calcium abundance from SMM-BCS data is described in a paper by Sylwester at al. (1996), which Dr. Sylwester kindly made available to us in advance of publication. Unfortunately, the area of overlap in time for our two studies is rather sparse. However, there are three active regions (AR) in common: using NOAA designations, AR 4787 and AR 4790 in April 1987 and AR 4811 in May 1987. For all three of these regions, the BCS data show calcium abundances near the mean values of the flare study. However, for AR 4787/90, there is one FCS quiescent active region spectrum for which Ne/O, Mg/O, and Fe/O are all more than 3-sigma below their respective mean values, and a second case where Mg/O and Fe/O are more than 3-sigma below the mean while Ne/O is at the 3-sigma lower limit. Again, for AR 4811, there is one active region spectrum for which Mg/O, Fe/O, and Ne/O are all more than 3-sigma below the mean; in the other quiescent active region spectrum from AR 4811, Mg/O, Fe/O, and Ne/O all appear to be systematically high (although the statistical significance is low). So we have uncovered no obvious correlation between active region and flare abundance variability, but this is not unexpected, given that the abundances in a given active regions can vary from day to day, and the two sets of data did not provide BCS flare and FCS active region samples on the same day. In any case, a larger joint sample is clearly needed.

b. Yohkoh SXT input for resonance scattering

SXT can provide a cross-check on the correct sense of center-to-limb effect in resonance scattering. Figure 5 shows a 2-d smoothed histogram of SXT relative intensities, from decompressed data numbers (see Tsuneta et al. 1991) in the Al/Mg/Mn filter, of the central bright portions of 10 active regions observed in 1994 as they transited the solar disk. The intensities are 3x3 summations of 5-arcsecond (half-resolution) pixels (thus yielding approximately 15-arcsec-squared "pixels" comparable to the FCS FWHM field of view), normalized to the intensity of the region's core at disk center. To be included in the sample, a region had to be visible for the full transit; 9 regions were stable or decaying, and one region was growing, which accounts for the overall East-West asymmetry. There is a clear trend of increasing signal at the limb, presumably due to longer effective lines of sight. The 15.01-A line of Fe XVII should be one of the brightest active region emission lines contributing to the

detector response in the Al/Mg/Mn filter. Since the 15.01-A line opacity scales roughly linearly with path length (the relationship is exact for the case of uniform electron density), one should expect maximum opacity at the limb, as found by the study of Schmelz et al. (1997), not a minimum, with the shortest effective path length, as found by Phillips et al. (1996).

c. SOHO Results

A number of SOHO scientists have been making studies of coronal and transition region abundances, but in general the results are still extremely preliminary. SUMER has identified new species in observations made above the pole, from transition region lines that tend to be overwhelmed by other stronger lines on the disk. CDS, SUMER, and UVCS are all making measurements looking for verifcation and the amplitude of the "FIP effect", i.e., the relative enhancement of low-FIP to high-FIP elements.

(1) CDS and MDI Observations

The CDS team has made a number of coronal abundance studies, but the data remain to be calibrated. In collaboration with Dr. Andrzej Fludra, the CDS Project Scientist, We have planned and carried out some specific joint CDS/MDI observations of quiet Sun in the MDI high-resolution field of view for 5-6 hours each day on 01 and 02 August 1996. (We had hoped for an active region target when we scheduled the observations, but the Sun declined to cooperate on that time.) For this first run, we chose to use the full range of both the Normal Incidence Spectrometer (NIS) (i.e., 309-380 A and 510-630 A) and the Grazing Incidence Spectrometer (GIS) (151-221, 256-338, 393-493, and 656-785 A), for a 1-arcmin-square field of view near disk center, reducing the area covered to be able to have the maximum possible redundancy in temperature coverage, available ions, and available emission lines, until more is known about the instrument calibration and the "hidden variables" in the line emissivities.
An SOI proposal was submitted to use the MDI high-resolution data on the photospheric magnetic and velocity fields, to search for correlations within these data sets or between these and future data sets.

(2) Preliminary UVCS Measurements

Dr. John Raymond of the UVCS team was kind enough to share some very preliminary streamer abundance results from UVCS, with permission to cite them in this report (priv. comm., Dec 1996). It should be possible to get absolute abundances from the UVCS data by considering either the collisionally excited part or the scattered part of the O VI line intensity (they are about equal, as determined from the 3:1 doublet ratio), relative to the Lyman gamma intensity. He finds that the average streamer spectrum, well fit by an isothermal model with T_e = 1.6 MK at 1.5 solar radii, yields a ratio for O/H that is consistent with the photospheric ratio (= 8.5e-4). If confirmed, this would imply that the low-FIP elements are in fact enhanced by about a factor of 4 and the high-FIP element oxygen is photospheric. On the other hand, O/H could be depleted below the photospheric value if there is a significant amount of cooler (T_e~0.5 MK) plasma. There is still much work to be done. For various lines, the atomic data used in the rate coefficients are being reconsidered, as are the ionization balance calculations for iron. However, in any case, it appears that He/H is depleted by at least a factor of 2 relative to the photospheric value, since He 1085 is not detected. Measurements of the absolute helium abundance in the corona are hard to come by. The most precise solar measurement of He/H previously available was that from the CHASE experiment on SpaceLab 2,

namely, He/H = 0.079 +/- 0.011. The meteoritic value, taken as the current best estimate of the solar photospheric value, is He/H = 0.098+/-0.008 (Anders & Grevesse 1989). Allen (1972) gives He/H = 0.085 in the photosphere. Although it will be difficult to see many lines in coronal holes, the UVCS team expects to be able to get an absolute abundance measurement there for at least oxygen. The contract PI was encouraged to join the UVCS abundance working group, led by Dr. Raymond, and has done so, being especially interested in correlating abundances in active regions with abundances in overlying streamers.

LESSONS LEARNED AND RECOMMENDATIONS

1. Coronal elemental abundances variations of at least a factor of 4 appear to be real. Although the variations cause complications in analysis, rather than "averaging over our ignorance", we need to understand the variability, ascertain what causes it, and make use of the information it contains. Ignoring the variability, in analyses of images or spectra, could lead to false results.

2. A larger sample of soft X-ray and EUV coronal measurements is needed to see if the coronal spectroscopic abundance data in fact have a different parent distribution than do the SEPs, as appears from the limted statistics here. A larger sample is also needed to make correlative studies of abundances in quiescent active regions, to understand when to expect abundance variability.

3. As much redundancy as possible should be included in the temperature coverage, to permit relative calibration of instrumental response, to allow for lines which turn out not to be as well understood as initially believed, and to provide for checks on opacity and ionization fractions, as well as study of element-to-element abundance variability.

4. For study of abundances in non-quiescent regions, post-flare regions, and long-duration events, the temperature distribution of the emission measure should be well sampled over the range from about 1 to about 20 MK. Most soft X-ray data alone do not have sufficient sensitivity at the cool end; most EUV data alone sample the high-temperature end too sparsely (leaving out the regime log T = 6.6-7.0) or not at all. The exciting new EUV data sets from SERTS and SOHO should be complemented by coordinated soft X-ray measurements, at least broad-band measurements from Yohkoh SXT as a sanity check on hotter plasma as the solar cycle picks up.

5. Different ionization balance calculations can affect qualitative as well as quantitative results. [For example, a change in FCS spectral line ratios can sometimes be interpreted as thermal evolution or abundance variation, depending on whether the Arnaud & Raymond (1992) or the Arnaud & Rothenflug (1985) calculations are used for the ion fractions. SMM-BCS authors have sometimes resorted to adoption of "empirical" ionization fractions to avoid apparent abundance variations during flare decays.] The recent iron ionization balance calculations by Arnaud & Raymond (1992) are being adopted by the SOHO community. Although they correct a known error in the earlier calculations by Arnaud & Rothenflug (1985), the FCS results appear to be more consistent with the older calculations for Fe XVII and Fe XVIII.

6. Resonance scattering results for Fe XVII at 15.01 A show that the

assumption that coronal lines are optically thin is not always valid. This is particularly true for bright iron resonance lines, where high elemental abundance coupled with large oscillator strength and large ionization fraction could lead to substantial opacity. In the EUV regime, most oscillator strengths are not as large as that for the 15.01-A Fe XVII line (viz., 2.66), but the factor of wavelength in the opacity more than compensates. One good EUV candidate for resonance scattering is the 284-A line of Fe XV, which figures importantly in SERTS and CDS spectra and in EIT and TRACE multilayer filters.

7. In addition to causing complications in the abundance studies and other analyses, resonance scattering may provide additional diangostic information on the source region. To obtain this information, one needs arcsecond pixel or better imaging of the source geometry at the same time as spectroscopic diagnostic information of on electron density from optically thin lines in the same temperature range as the resonantly scattered line, to determine the appropriate filling factor of the emission.

8. To study transient brightenings and hot components in active regions, good imaging data are needed in conjunction with good spectral resolution and temperature coverage. What one really needs are high-cadence, high-spatial-resolution images in conjunction with moderate-cadence, high-resolution EUV and soft X-ray plasma diagnostics at the same time. A good start on most of the needed information could be gotten from coordinated measurements from SERTS, CDS, EIT, TRACE, and Yohkoh SXT.

PUBLICATIONS SUPPORTED BY THIS CONTRACT

The Composition of a Coronal Active Region: Waljeski, K., Moses, D., Dere, K.P., Saba, J.L.R., Strong, K.T., Webb, D.F., and Zarro, D.M. 1994, ApJ, 429, 909

Implications of Coronal Abundance Variations: Saba, J.L.R. and Strong, K.T. 1994, Proceedings of the Kofu Symposium, ''New Look at the Sun with Emphasis on Advanced Observations of Coronal Dynamics and Flares -- What Do We See with Yohkoh and Nobeyama Radioheliograph,'' eds. S. Enome and T. Hirayama, Nobeyama Radio Observatory Report No. 360, 1994

Looking for the FIP Effect in EUV Spectra: Examining the Solar Case: Haisch, B.M., Saba, J.L.R., and Meyer, J.-P. 1996, Astrophysics in the Extreme Ultraviolet, eds. S. Bowyer and R.F. Malina, Kluwer, p 511.

Anomalous Coronal Neon Abundances in Quiescent Solar Active Regions: Schmelz, J.T., Saba, J.L.R., Ghosh, D., and Strong, K.T. (1996), Ap.J., In Press.

Investigating the Effect of Opacity in Soft X-Ray Spectral Lines Emitted by Solar Coronal Active Regions: Schmelz, J.T., Saba, J.L.R., Chauvin, J.C., and Strong, K.T. (1997), Ap.J., In Press.

Ne/O, Mg/O, and Fe/O Abundances Derived from Spectroscopic and SEP Analysis: Schmelz, J.T., Saba, J.L.R., and Islam, B., (1997) Adv. Space Res., Submitted.

Resonance Scattering of Fe XVII: II. Intercomparison of Data and Theory: Saba, J.L.R., Schmelz, J.T., Bhatia, A.K., and Strong, K.T. (1997), Ap.J.,

In Prep.

PRESENTATIONS OF RESULTS OF THE ABUNDANCE STUDY

SMM Flat Crystal Spectrometer Measurements of Solar Active Region Abundances: Variations on the FIP theme: Saba, J.L.R. and Strong, 24th meeting of the Solar Physics Division of the A.A.S., Stanford, California, 13-16 July 1993.

Is Hydrogen Acting Like a High FIP or a Low FIP Element in the Solar Corona? Schmelz, J.T., Strong, K.T., and Lemen, J.R. (1993), BAAS, 25, 1201.

Implications of Coronal Abundance Variations: Saba, J.L.R. and Strong, K.T., Kofu Symposium on a "New Look at the Sun with Emphasis on Advanced Observations of Coronal Dynamics and Flares -- What Do We See with Yohkoh and Nobeyama Radioheliograph", Kofu, Japan, 6-10 September 1993.

An Abundance of New Information for Astrophysics from the Solar Corona: J.L.R. Saba, Laboratory for Astronomy & Solar Physics seminar at Goddard Space Flight Center, 30 September 1993.

A Reexamination of the Impact of Resonance Scattering on FCS Active Region Abundance Measurements: talk at the joint American Geophysical Union--American Astronomical Society/ Solar Physics Division Meeting in Baltimore, Maryland, May 1994.

Spectroscopic Measurements of Element Abundances in the Solar Corona: Variations on the FIP Theme: Saba, J.L.R., invited review at 30th Assembly of the Committee on Space Research (COSPAR), Hamburg, Germany, July 1994.

Absolute Abundances of Flaring Coronal Plasma Derived from SMM Spectral Observations: Schmelz, J.T. (1994), EOS, 75, (16)290.

Abundance Variations from SMM Spectroscopic Observations of Non-Flaring Plasma: Ghosh, D. and Schmelz, J.T. (1995), BAAS, 27, 962.

Testing the Optically Thin Assumption for Soft X-Ray Spectral Lines of the Solar Corona: Chauvin, J.C. and Schmelz, J.T. (1995), BAAS, 27, 967.

Ne/O, Mg/O, and Fe/O Abundances Derived Spectroscopically for Coronal Plasma: Schmelz, J.T., Miller, T.R., and Saba, J.L.R. (1995), BAAS, 27, 967

Opacity Effects in Soft X-Ray Spectral Lines of the Solar Corona: Schmelz, J.T. and Chauvin, J.C. (1996), BAAS, 28, 874.

Ne/O, Mg/O, and Fe/O Abundances Derived from Spectroscopic and SEP Analysis: Islam, B. and Schmelz, J.T. (1996), BAAS, 28, 941.

REFERENCES

Allen, C.W. 1973, Astrophysical Quantities, 3rd ed, The Athlone Press
Anders, E., and Grevesse, N. 1989, Geochimica et Cosmochimica Acta, 53, 197
Arnaud, M. & Raymond, J. 1992, ApJ, 398, 394
Arnaud, M. & Rothenflug, R. 1985, ApJS, 60, 425
Bhatia, A.K. & Doschek, G.A. 1992, Atomic Data Nucl. Data, 52, 1
Cornille, M., Dubau, J., Faucher, P., Bely-Dubau, F., and Blancard, C. 1994 A&S Suppl. Ser., 105, 77
McKenzie, D.L. & Feldman, U. 1992 ApJ, 389, 764
Mewe, R., Gronenschild, E.H.B.M. & van den Oord, G.H.J. 1985, A&AS 62, 197
Meyer, J.-P., 1985, ApJS 57, 173
Murphy, R.J., Ramaty, R., Kozlovsky, B. & Reames, D.V. 1991, ApJ, 371, 793
Phillips, K.J.H., et al. 1995 Adv. Space Res., 17, 7(3)7
Phillips, K.J.H., Greer, C.J., Bhatia, A.K., & Keenan, F.P. 1996, ApJ, 469, L57
Reames, D.V. 1995, Adv. Space Res., 15, (7)41
Saba, J.L.R., Schmelz, J.T., Strong, K.T., & Bhatia, A.K. 1997, in prep.
Saba, J.L.R. & Strong, K.T. 1991, ApJ, 375, 789
Saba, J.L.R. & Strong, K.T. 1991, Adv. Space Res., 11, (1)117
Saba, J.L.R. & Strong, K.T. 1992, Proceedings of the first SoHO Workshop, Annapolis, Maryland, ESA SP-348, 347
Saba, J.L.R. & Strong, K.T. 1993, Adv. Space Res., 13, (9)391
Schmelz, J.T. 1993, ApJ, 408, 373
Schmelz, J.T. & Fludra, A. 1993, Adv. Space Res., 13, (9)325
Schmelz, J.T., Saba, J.L.R. & Strong, K.T. 1992, ApJ, 398, L115
Schmelz, J.T., Saba, J.L.R., Chauvin, J.C. & Strong, K.T. 1997,
Schmelz, J.T., Saba, J.L.R., & Islam, B. 1997, Adv. Space Res., in press
Strong, K.T., Lemen, J.R. & Linford, G.A. 1991, Adv. Space Res., 11, (1)151
Shemi, A. 1991, MNRAS, 251, 221
Sylwester, J., Lemen, J.L., Bentley, R.D., Fludra, A. & Zolcinski, M.C. 1996, ApJ, in press
Tsuneta, S. et al. 1991, Sol. Phys., 136, 37.
Veck, N.J. & Parkinson, J.H. 1981, MNRAS, 197, 41
Waljeski, K., Moses, D., Dere, K.P., Saba, J.L.R., Strong, K.T., Webb, D.F., and Zarro, D.M. 1994, ApJ, 429, 909

Table 1

Date	Time	AR	Temp (MK)	Mg/O	Ne/O	Fe/O
86 May 20	00:19-01:12	4729	$2.66^{+.16}_{-.26}$	0.19 ± 0.05	0.29 ± 0.03	0.12 ± 0.007
86 May 21	14:02-14:55	4731	$2.92^{+.07}_{-.10}$	0.20 ± 0.03	0.13 ± 0.01	0.11 ± 0.014
86 May 23	02:11-03:07	4731	$2.82^{+.10}_{-.10}$	0.19 ± 0.03	0.07 ± 0.01	0.11 ± 0.008
86 May 24	04:54-05:50	4731	$2.88^{+.07}_{-.10}$	0.26 ± 0.05	0.14 ± 0.02	0.12 ± 0.012
87 Apr 11	22:26-23:21	4787	$2.95^{+.10}_{-.07}$	0.21 ± 0.04	0.20 ± 0.02	0.11 ± 0.008
87 Apr 13	01:08-02:03	4787/90	$3.09^{+.04}_{-.07}$	0.35 ± 0.05	0.19 ± 0.02	0.12 ± 0.008
87 Apr 14	14:50-15:45	4787/90	$3.05^{+.07}_{-.07}$	0.18 ± 0.02	0.14 ± 0.01	0.10 ± 0.019
87 Apr 15	15:58-16:54	4787/90	$3.47^{+.04}_{-.04}$	0.13 ± 0.01	0.13 ± 0.01	0.07 ± 0.009
87 Apr 15	23:22-24:17	4787/90	$3.05^{+.07}_{-.04}$	0.35 ± 0.05	0.18 ± 0.03	0.10 ± 0.016
87 Apr 19	14:41-15:10	4787/90	$3.09^{+.04}_{-.07}$	0.11 ± 0.01	0.14 ± 0.01	0.05 ± 0.007
87 May 26	01:12-02:08	4811	$3.59^{+.08}_{-.08}$	0.06 ± 0.01	0.08 ± 0.02	0.05 ± 0.012
87 May 29	18:43-19:39	4811	$3.02^{+.15}_{-.33}$	0.31 ± 0.11	0.43 ± 0.12	0.18 ± 0.017
87 Jun 13	02:40-03:36	SN50	$2.75^{+.16}_{-.24}$	0.26 ± 0.06	0.06 ± 0.01	0.14 ± 0.024
87 Nov 27	16:20-17:17	4891	$2.79^{+.06}_{-.13}$	0.14 ± 0.02	0.09 ± 0.01	0.08 ± 0.012
87 Nov 29	20:07-21:06	4891	$2.88^{+.07}_{-.07}$	0.16 ± 0.09	0.10 ± 0.03	0.21 ± 0.016
87 Dec 06	16:58-18:01	4901	$3.43^{+.12}_{-.06}$	0.40 ± 0.06	0.18 ± 0.03	0.09 ± 0.008
87 Dec 07	10:15-11:17	4901	$2.92^{+.10}_{-.10}$	0.79 ± 0.43	0.47 ± 0.10	0.34 ± 0.078
87 Dec 07	14:48-16:01	4901	$2.99^{+.10}_{-.13}$	0.17 ± 0.04	0.21 ± 0.03	0.09 ± 0.009
87 Dec 08	03:32-04:34	4901	$2.72^{+.19}_{-.46}$	0.22 ± 0.06	0.26 ± 0.03	0.11 ± 0.012
87 Dec 08	09:49-10:51	4901	$3.20^{+.07}_{-.11}$	0.14 ± 0.02	0.23 ± 0.03	0.07 ± 0.007
87 Dec 08	16:06-17:08	4901	$3.05^{+.07}_{-.14}$	0.17 ± 0.04	0.27 ± 0.03	0.07 ± 0.009
87 Dec 09	03:06-04:08	4901	$3.13^{+.07}_{-.04}$	0.25 ± 0.03	0.14 ± 0.01	0.07 ± 0.014
87 Dec 09	07:48-08:50	4901	$2.02^{+.56}_{-.43}$	0.11 ± 0.03	0.16 ± 0.02	0.05 ± 0.007
87 Dec 10	02:39-03:40	4901	$3.02^{+.11}_{-.11}$	0.11 ± 0.03	0.20 ± 0.02	0.06 ± 0.011
87 Dec 10	10:31-11:31	4901	$2.79^{+.20}_{-.39}$	0.06 ± 0.02	0.15 ± 0.02	0.05 ± 0.009
87 Dec 11	02:13-03:13	4901	$3.05^{+.07}_{-.03}$	0.09 ± 0.01	0.12 ± 0.01	0.08 ± 0.015
87 Dec 11	10:04-11:04	4901	$3.24^{+.06}_{-.04}$	0.30 ± 0.04	0.16 ± 0.02	0.10 ± 0.050
87 Dec 13	09:10-10:09	SELimb	$2.79^{+.10}_{-.09}$	0.15 ± 0.02	0.16 ± 0.01	0.08 ± 0.053
87 Dec 15	03:34-04:31	4906	$3.02^{+.07}_{-.07}$	0.13 ± 0.02	0.16 ± 0.01	0.05 ± 0.013
87 Dec 16	07:49-08:46	4906	$3.09^{+.07}_{-.10}$	0.16 ± 0.02	0.15 ± 0.01	0.09 ± 0.012
87 Dec 18	03:46-04:42	4906	$2.54^{+.21}_{-.68}$	0.14 ± 0.03	0.10 ± 0.02	0.07 ± 0.011
87 Dec 18	06:54-07:50	4906	$2.92^{+.28}_{-1.33}$	0.58 ± 0.24	0.13 ± 0.05	0.07 ± 0.020
87 Dec 20	09:07-10:03	4906	$3.72^{+.27}_{-.48}$	0.05 ± 0.02	0.09 ± 0.03	0.03 ± 0.016
Mean				0.21 ± 0.016	0.17 ± 0.006	0.106 ± 0.004
Mean *				0.19 ± 0.004	0.152 ± 0.004	0.134 ± 0.004

* Reames (1995)

FIGURE CAPTIONS

Fig. 1: Illustration of FCS spectral differences due to coronal abundance variations.

Shown are two examples of the lowest energy FCS spectrum for two different solar active regions during periods of queiscence. The regions have very similar temperatures (about Log T = 6.5) as determined from the ratio of the Fe XVIII line at 14.22 A (line (d) in upper plot) to the Fe XVII line at 16.78 A (not shown). The spectral line strengths are very similar in each spectrum except for the three lines from the helium-like neon triplet at the far left, denoted (a), (b), and (c) in the upper plot. Those in the first spectrum are significantly stronger than their counterparts in the second spectrum.

Fig. 2: Evidence for resonance scattering in FCS active region data.

Figure 2a shows the flux ratio of the unaffected 16.78-A line of Fe XVII to the most-affected 15.01-A line for the FCS data (crosses) and the theoretical predictions (solid line for Log T = 6.5 and dashed lines for Log T = 6.4 and 6.6, a range which covers those found for the quiescent active regions in our study). The data points are plotted in order of increasing distance from Sun center and are all significantly above the expected theoretical values, consistent with 15.01-A photons being scattered out of the line of sight. For comparison, Figure 2b shows the same type of plot, with the 15.25-A line substituted for the 15.01-A line. The 15.25-A line has an opacity less than 25% that of the 15.01-A line, so it should not show significant opacity effects under normal active region conditions. The data and theory agree, indicating that these two lines are well explained with an optically thin approximation.

Fig. 3: Effect of iron ionization balance calculations on EM/T curve overlays for quiescent FCS active region spectrum.

Top panel: An isothermal distribution results if the Arnaud & Rothenflug (1985) ionization fractions are used (with an iron abundance of 3.2e-5, the meteoritic value). The one-sigma emission measure bands for the O VIII, Ne IX, and Mg XI resonance lines (all shown with dotted curves), and for the Fe XVII 16.78-A line (dot-dash curves) and the Fe XVIII 14.22-A line (dashed curves) all intersect in a single temperature solution.

Bottom panel: If the newer ionization fraction calculations of Arnaud & Raymond (1992) are used, the results are more complex; in particular, no single isothermal solution can be found.

Atomic data from Bhatia & Doschek (1992) are used for the Fe XVII lines at 15.25 A and 16.78 A, and atomic data from McKenzie & Feldman (1992) for Fe XVIII at 14.22 A.

Fig. 4: Comparison of relative abundances for SEP and FCS data. (After Figure 1 in Schmelz et al. 1997.)

The left panel shows histogram distributions of Mg/O, Ne/O, and Fe/O for the SEP measurements of Reames (1995). (Note that the variance of the SEP Fe/O distribution is much larger than for Mg/O or Ne/O.) The right panel gives the histogram distribution of relative abundances for the sample of 33 FCS spectra from quiescent active regions. The dispersion in relative abundances is much greater in the FCS than in the SEP data. A possible explanation is that the SEP data come from averages over larger spatial and temporal scales.

Fig. 5: SXT input for cross-checking sense of center-to-limb effect in resonance scattering.

Shown is a 2-d smoothed histogram of SXT relative intensities, from decompressed data numbers (see Tsuneta et al. 1991) in the Al/Mg/Mn filter, of the central bright portions of 10 active regions as they transited the solar disk. The intensities are 3x3 summations of 5-arcsec (half-resolution) pixels (thus yielding approximately 15-arcsec-squared "pixels" comparable to the FCS FWHM field of view), normalized to the intensity of the region's core at disk center. To be included in the sample, a region had to be visible for the full transit; 9 regions were stable or decaying, and one region was growing, which accounts for the overall East-West asymmetry. There is a clear trend of increasing signal at the limb, presumably due to longer effective lines of sight.

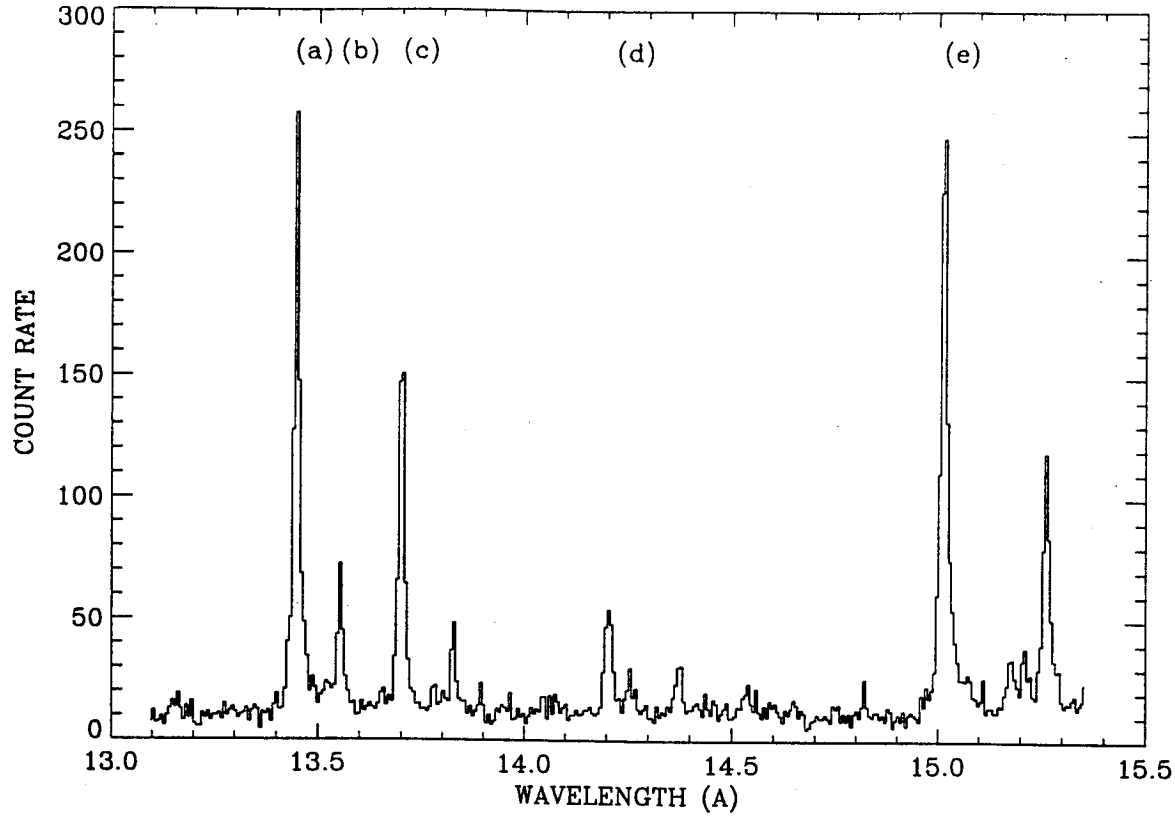
(a) (b) (c)
(d)
(e)
COUNT RATE
300
250
200
150
100
50
0
13.0
13.5
14.0
14.5
15.0
15.5
WAVELENGTH (A)

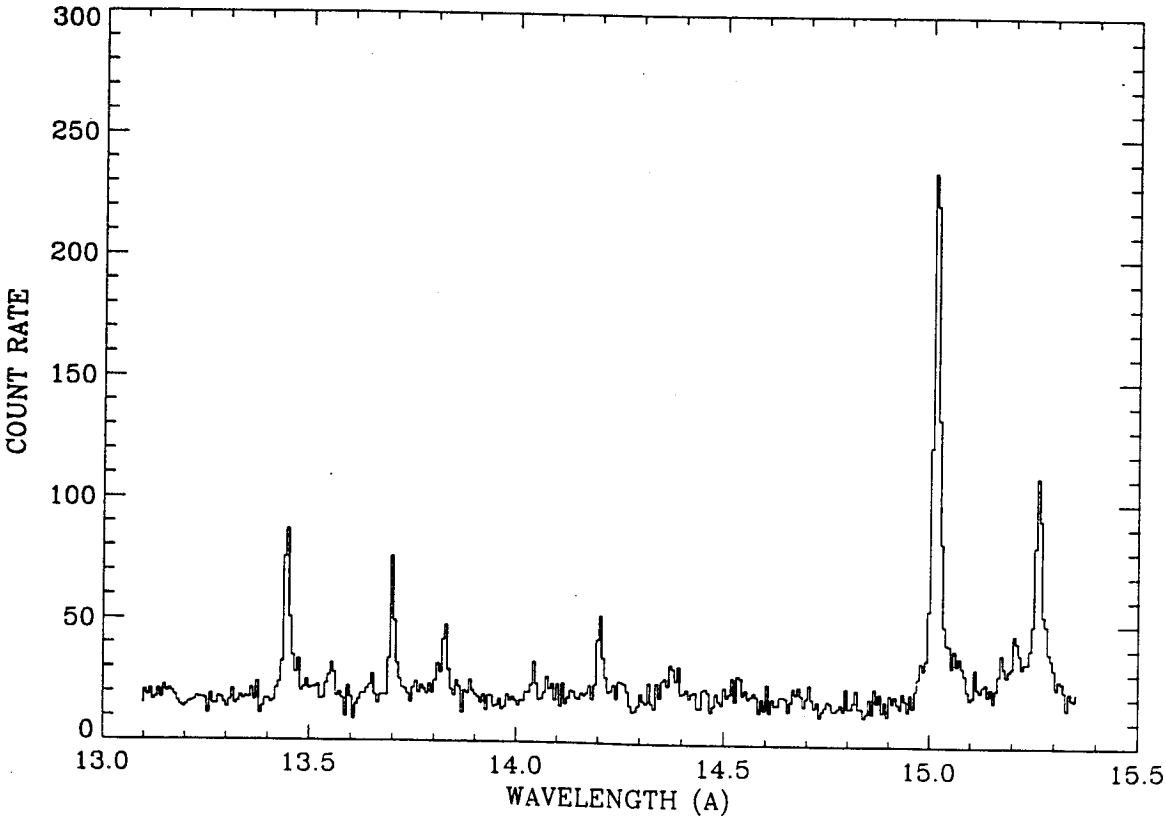
COUNT RATE
300
250
200
150
100
50
0
13.0
13.5
14.0
14.5
15.0
15.5
WAVELENGTH (A)

Figure 1

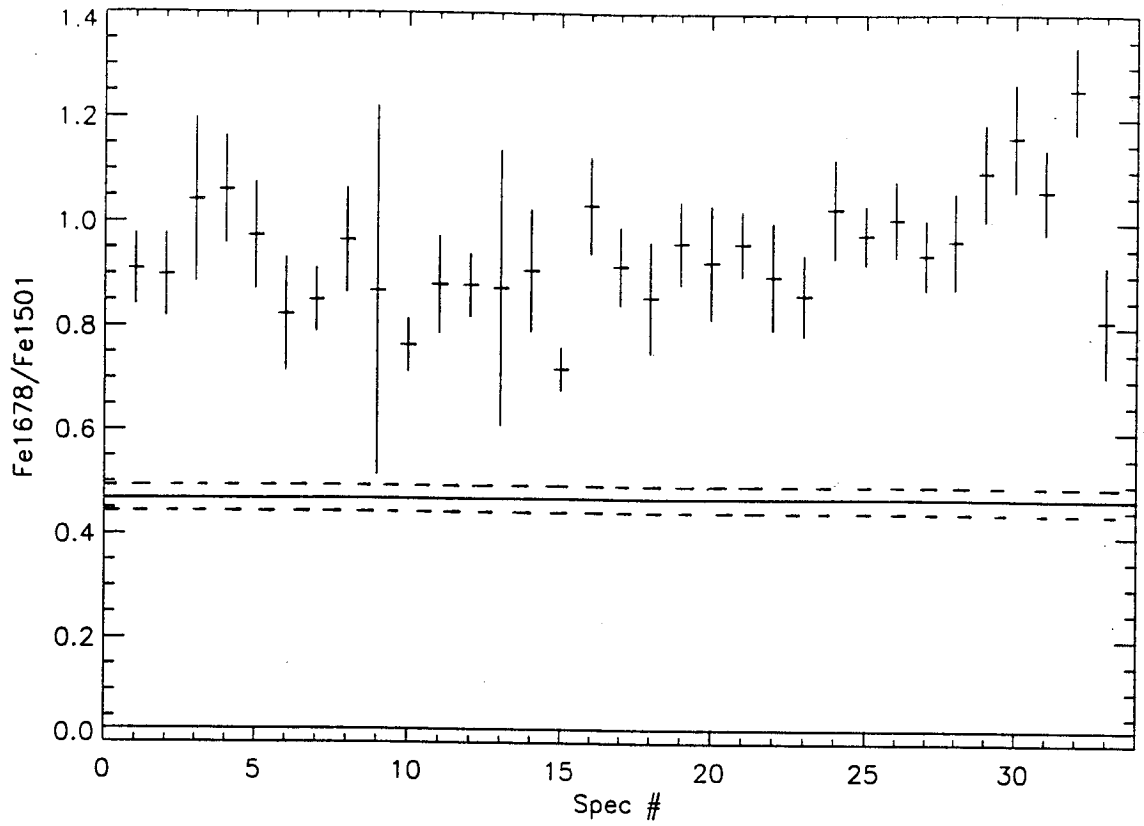
Fe1678/Fe1501
1.4
1.2
1.0
0.8
0.6
0.4
0.2
0.0
0
5
10
15
20
25
30
Spec #

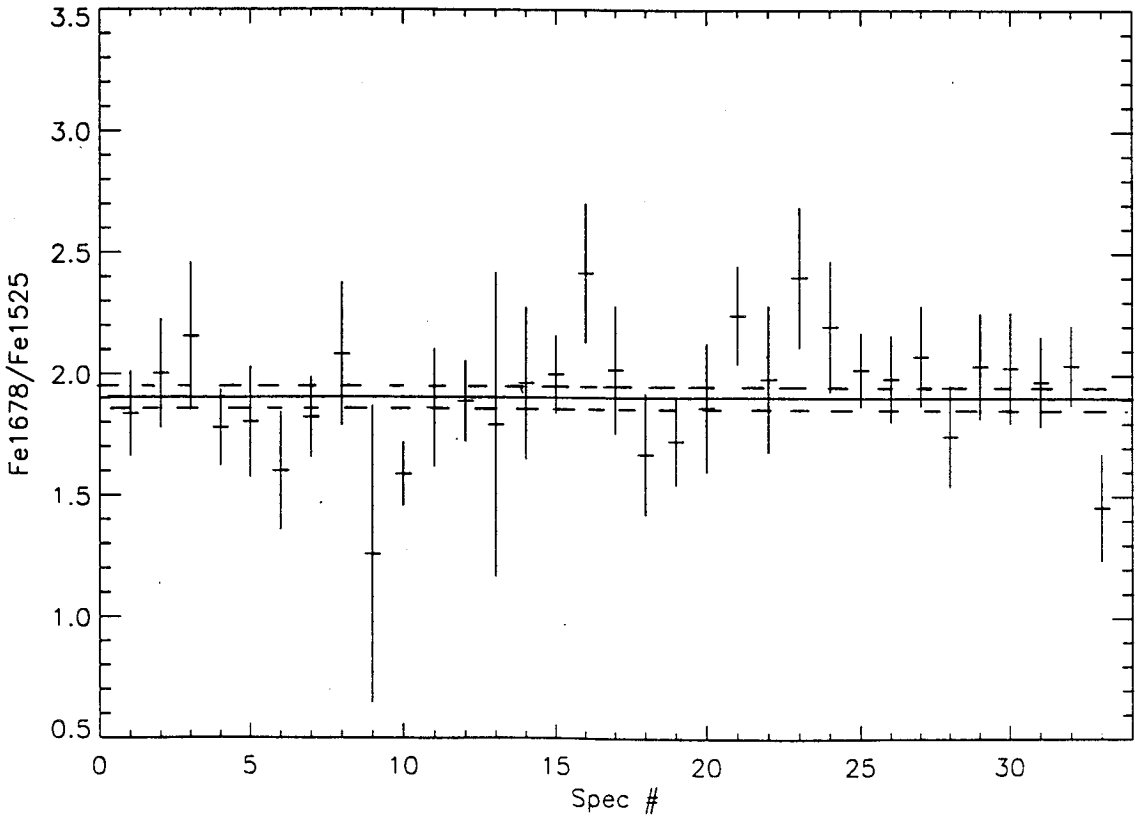
Fe1678/Fe1525
3.5
3.0
2.5
2.0
1.5
1.0
0.5
0
5
10
15
20
25
30
Spec #

Figure 2

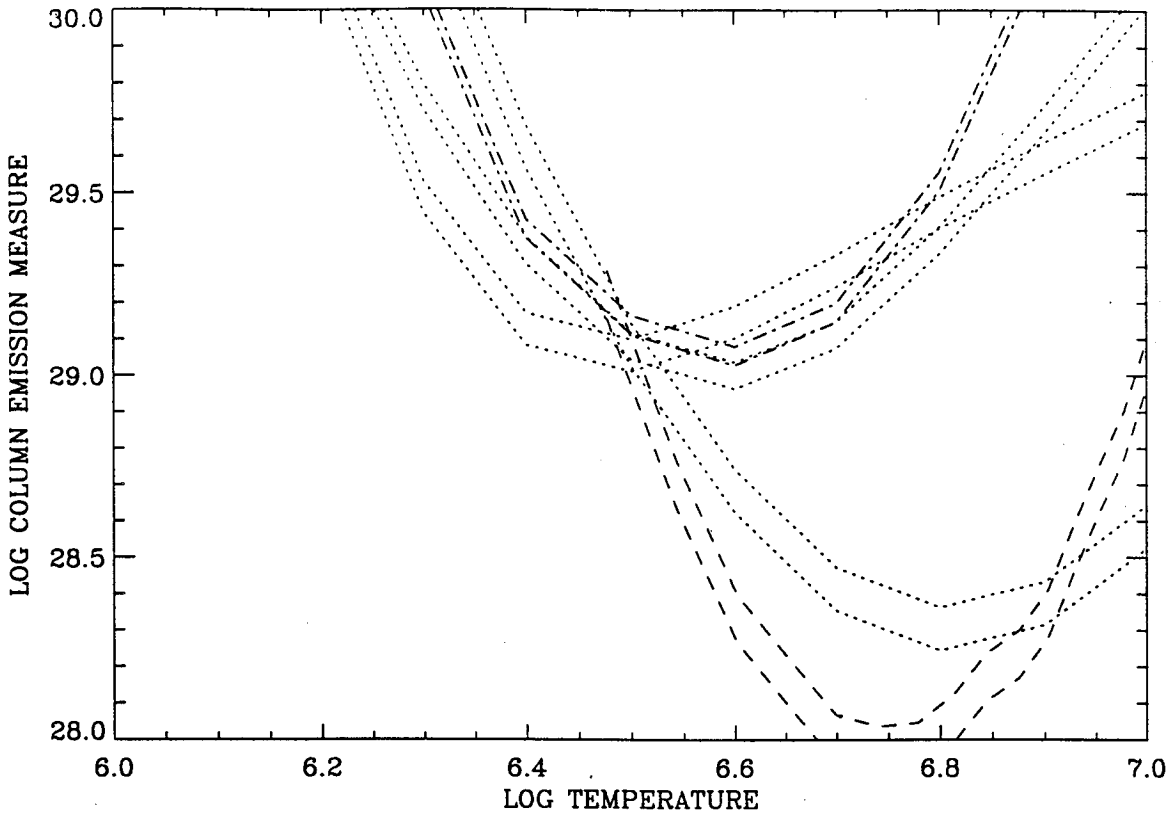
30.0
29.5
29.0
28.5
28.0
LOG COLUMN EMISSION MEASURE
6.0
6.2
6.4
6.6
6.8
7.0
LOG TEMPERATURE

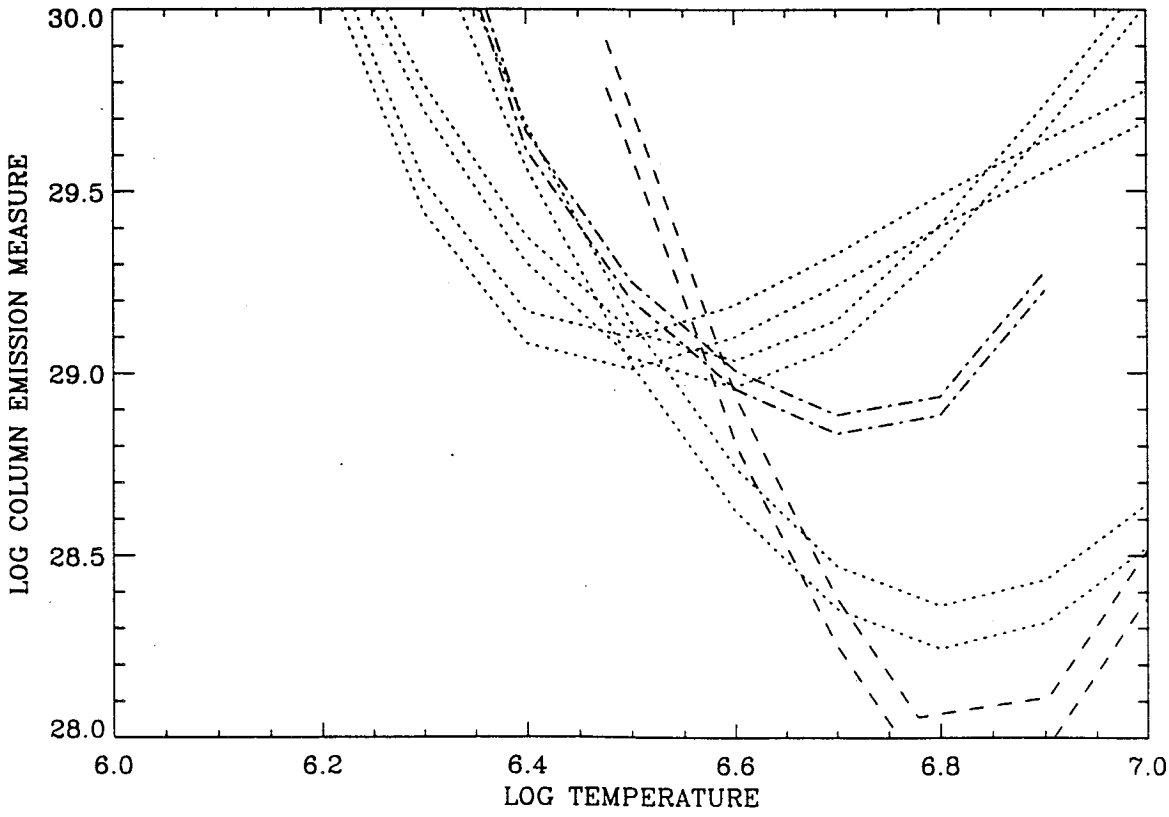
30.0
29.5
29.0
28.5
28.0
LOG COLUMN EMISSION MEASURE
6.0
6.2
6.4
6.6
6.8
7.0
LOG TEMPERATURE

Figure 3

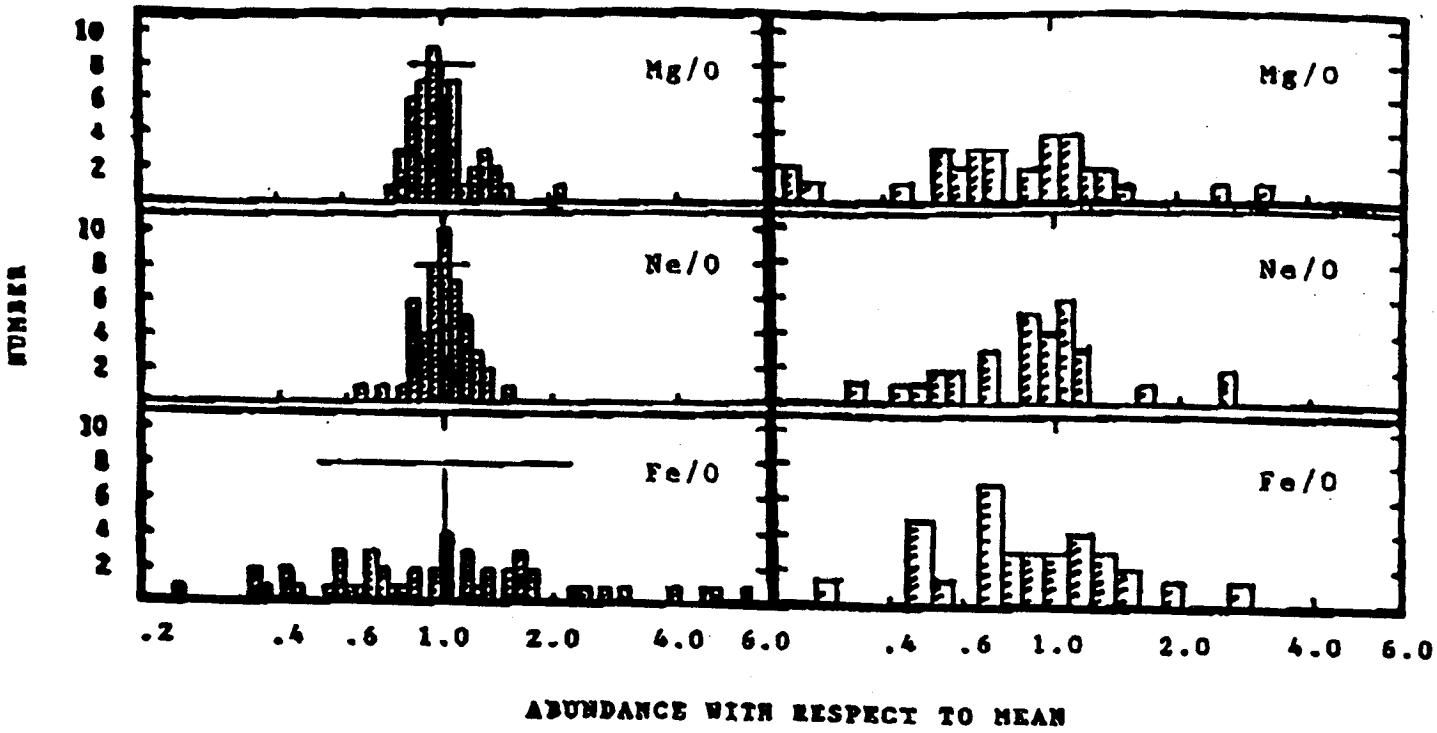
Mg/O
Mg/O
Ne/O
Ne/O
Fe/O
Fe/O
10
8
6
4
2
.2
.4
.6
1.0
2.0
4.0
6.0
ABUNDANCE WITH RESPECT TO MEAN

Figure 4

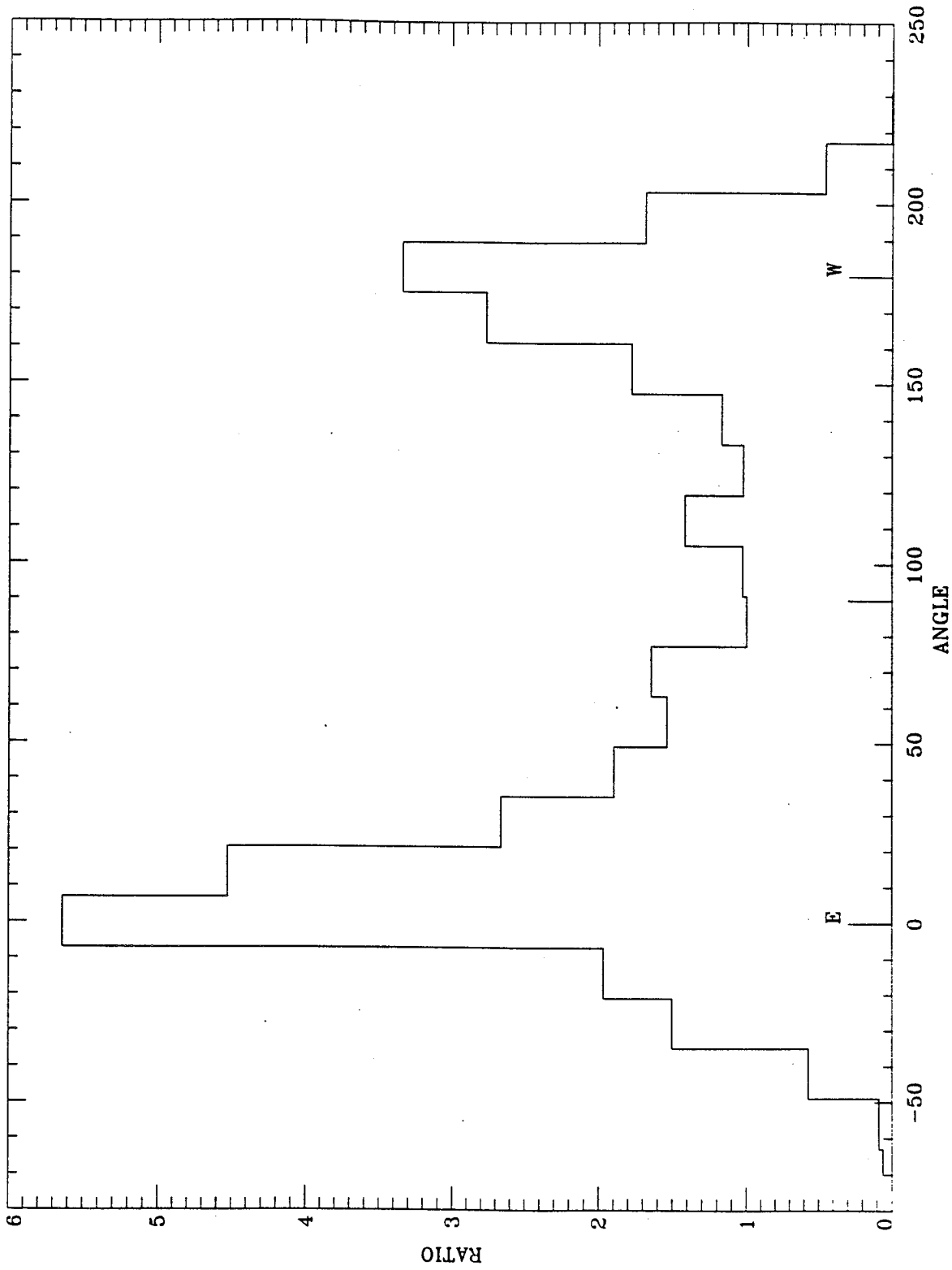

Figure 5

NASA REPORT DOCUMENTATION PAGE
(IN LIEU OF NASA FORM 1626)

1. REPORT NO.	2. GOVERNMENT ACCESSION NO.	3. RECIPIENT'S CATALOG NO.
4. TITLE AND SUBTITLE Coronal Abundances and their Variation: Final report - for contract period of performance: June 1993 - December 1996		5. REPORT DATE 12 December 1996 6. PERFORMING ORGANIZATION CODE: O/H1-12
7. AUTHOR(S) J. L. R. Saba (LMPARL) and J. T. Schmelz (U. Memphis)		8. PERFORMING ORGANIZATION REPORT NO:
9. PERFORMING ORGANIZATION NAME AND ADDRESS Lockheed Martin Palo Alto Research Laboratory Solar & Astrophysics Lab., O/H1-12, Bldg 252 3251 Hanover Street, Palo Alto Ca. 94304		10. WORK UNIT NO. 11. CONTRACT OR GRANT NO. NASW-4814
12. SPONSORING AGENCY NAME AND ADDRESS NASA Headquarters Solar Physics Branch Space Physics Division Washington, D.C. 20546		13. TYPE OF REPORT AND PERIOD COVERED Final report, covering period June 1993 - December 1996 14. SPONSORING AGENCY CODE NASA HQ/ CODE SR
15. SUPPLEMENTARY NOTES		

16. ABSTRACT
This contract supported the investigation of elemental abundances in the solar corona, principally through analysis of high-resolution soft X-ray spectra from the Flat Crystal Spectrometer on NASA's Solar Maximum Mission. The goals of the study were a characterization of the mean values of relative abundances of elements accessible in the FCS data, and information on the extent and circumstances of their variability. This the Final Report, which summarizes the data analysis and reporting activities during the period of performance of the contract, June 1993 to December 1996.

17. KEY WORDS (SUGGESTED BY AUTHOR(S)) X-Ray, Spectra, Corona, Composition		18. DISTRIBUTION STATEMENT Space Science, Solar Physics		
19. SECURITY CLASSIF. (OF THIS REPORT) None	20. SECURITY CLASSIF. (OF THIS PAGE) None	21. NO OF PAGES 26	22. PRICE	

For sale by: Superintendent of Documents, U.S. Government Printing Office, Washington, D.C. 20402-0001